JACS
JOURNAL OF THE AMERICAN CHEMICAL SOCIETY

Communication

pubs.acs.org/JACS

# Biocompatible, Functional Spheres Based on Oxidative Coupling Assembly of Green Tea Polyphenols

Zhenhua Chen,[†,‡] Caihong Wang,[†] Junze Chen,[†] and Xudong Li*[,†]

[†]National Engineering Research Center for Biomaterials, Sichuan University, Chengdu 610064, P. R. China

[‡]College of Pharmacy, Liaoning Medical University, Jinzhou, 121001, P. R. China

Supporting Information

**ABSTRACT:** Green luminescent, monodisperse, smooth, porous and hollow spheres were simply prepared by $Cu^{2+}$ and temperature mediated oxidative coupling assembly of green tea polyphenols in water. These polymeric tea polyphenol spheres are GSH responsive, acid resistant but alkali-responsive, ideally used as platform for controlled delivery of functional guests.

Encapsulation of functional guests within micro/nanosized hosts is of great interest in the fields of catalysis, cosmetics, medical diagnostics, drug delivery and materials science.[1] Among various hosts/carriers, such as micelles,[2] organogels,[3] dendrimers[4] and inorganic particles,[5] spheres with porous or hollow structure are always attractive because their void space permits encapsulating large quantities of guests. Molecular design of stimuli-responsive functional spheric systems, e.g., pH- or redox-responsive,[2,3,5] is now a key theme in the biomedical field for effective loading and smart release of guest molecules, and a simple preparation protocol is highly acclaimed to avoid any pollutants or even toxic species for various biomedical purposes. So far, most of the current porous/hollow spheric systems are derived from nonrenewable petrochemical sources. Herein, we demonstrate a simple method to fabricate functional spheres with flexible structural control from naturally reproducible and edible green tea.

Green tea polyphenols (TP) is a group of polyphenol compounds extracted from green tea, accounting for up to 30% of the plant's dry leaf weight, and collectively referred to as catechins (main components illustrated in Figure 1A). The beneficial health effects of TP or by ingesting green tea have been shown to reduce the risk of chronic and degenerative diseases,[6] and restrain human stone formation.[7] The unique physicochemical properties and biological activities of TP have been well documented.[8] The vicinal di- or trihydroxy structures of TP contribute to metal chelation[9] and antioxidative activities, but they also make catechins susceptible to air oxidation. Autoxidation, enzymatic and chemical oxidation are ubiquitous, e.g., forming dehydrodiepicatechins, proanthocyanidins, theaflavins and thearubigins in plant browning, green tea and tea fermentation.[10] The extensive research of the reactive activities[11] has had a major impact on our knowledge of oxidizing processes and catechin derivatives,[12] and also drives the development of new strategies and methodologies for the elaboration into further chemically transformed and complex oligo/polymeric polyphenolic assemblies.[13]

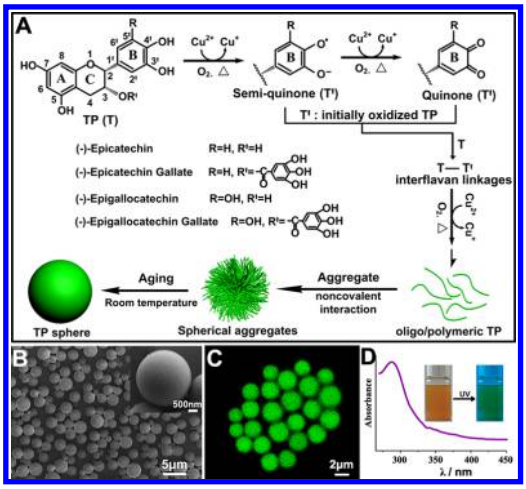


**Figure 1.** (A) Schematic illustration of temperature and Cu(II) mediated oxidative assembly of TP, and characterization of CT-1 spheres obtained in the presence of 70 mM $Cu^{2+}$ at 100 °C: (B) SEM, (C) CLSM and (D) UV−vis spectrum and well-dispersed spheres in water.

The present strategy simply involves copper (II, $Cu^{2+}$) and temperature mediated oxidative coupling assembly of TP to prepare biocompatible smooth, porous and hollow spheres. As schematic in Figure 1A, at heating condition and ambient atmosphere, the catechol and pyrogallol groups of (epi)-catechins and (epi)(gallo)catechins gallates (T) are initially converted to corresponding highly reactive semiquinones and quinones (T′).[8c,11] The subsequent coupling formation of interflavan linked dehydrodicatechins (T-T′) proceeds primarily through nucleophilic addition involving a quinone[10−12] but also possibly through coupling reaction involving a semiquinone radical.[11a,12b] This process is mediated by redox cycling of $Cu^{2+}/Cu^{+}$ couple and coordination of Cu to catechins.[9,11b,c,12a] Cu(II) acts as catalysts in plant browning via copper-containing glycoproteins[10a] and in oxidation polymerization of aromatic compounds,[14] and is shown to accelerate the oxidation coupling TP transformation.[9,11,12a] Successive coupling of catechins and oxidized catechins extends the linkage of oligo/polymeric TP. Finally, when the temperature reduces to room temperature (RT), these extending oligo/polymeric TP gradually aggregate and assemble via

**Received:** November 20, 2012
**Published:** March 7, 2013






dx.doi.org/10.1021/ja311374b | J. Am. Chem. Soc. 2013, 135, 4179−4182

noncovalent interaction into yellowish spheric precipitates, which obey the minimum surface energy principle.

The experimental procedures are given in Supporting Information. The precipitates obtained in the presence of 70 mM $Cu^{2+}$ at 100 °C, sample CT-1, are separate, smooth spheres with the size range of 1−3 μm (Figure 1B). The confocal laser scanning microscopy (CLSM) image (Figure 1C) reveals the green luminescent property of these microspheres (MSs). The UV−vis spectrum (Figure 1D) is similar to that of TP with an maximum absorbance at ∼280 nm,[8b] confirming the absence of theaflavins formed by condensation reactions of B-rings of gallocatechins and their gallates as their benzotropolone structure has characteristic absorbance peaks at 380 and 460 nm.[10c] This indicates that the majority of the original TP structure was retained in TP MSs, but this feature was also observed in the case of the C4−C8(6) linked structure such as in tea proanthocyanidins,[10b] $H_2O_2$ oxidative tea oxypolymers,[12d] and polymeric TP from postfermented tea,[12f] as well as in all C6′−C8 and C3′(4′)−O−C8 linked dimers of enzymatically oxidized catechin solutions.[12b] Correspondingly, the photoluminescence spectrum (Figure S1) records an emission peak at ∼310 nm. The inset shows that CT-1 MSs are well dispersive in water. Dynamic light scattering (DLS) and zeta potential results validate the good colloidal stability due to the charge repulsion of the spheres (Figure 1D). The negative surface charge of −25.5 mV indicates the presence of carboxyl groups in the oligo/polymeric TP MSs, suggesting the oxygenative cleavage of the catechol B-ring of epicatechin.[12f] Physicochemical analyses further provide the relevant molecular and structural information.

FTIR spectra (Figure S2) show that the oxidation and Cu-coordination leads to broadening and shifting of TP adsorptions centered at 3393−3320 $cm^{-1}$, shifting of TP C═O adsorptions from 1637 to 1620 $cm^{-1}$, existence of a sharp adsorption at 1530 $cm^{-1}$, obviously stronger 1450 $cm^{-1}$, broadening and shifting of 1355 to 1345 $cm^{-1}$ in the spectrum of CT-1 MSs. The reduced intensity of absorptions in the range of 620−900 $cm^{-1}$ further indicated the modifications of the aromatic ring moieties. The adsorption at 1530 $cm^{-1}$ is assigned to C−C aromatic rings, while the adsorption at 1100 $cm^{-1}$ is due to the symmetric vibrations of the ether bond in CT-1 MSs.[12b,15] Compared with pure TP, a very strong fluorescence background in the range of 1800−1000 $cm^{-1}$ exists in Raman spectrum of CT-1 MSs (Figure S3), showing that they are chemically complex products. But a new, strong absorption at 956 $cm^{-1}$ due to C−O vibrations is detected.[15b] Other new bands in the low wavenumber region at 586 and 428 $cm^{-1}$ further confirm the formation of oligo/polymeric TP.[9a] X-ray diffraction analysis (Figure S4) confirms the amorphous feature of CT-1 MSs, different with those coordination polymerized metal−organic spheres (MOSs) which usually have a highly crystallized structure.[1b] Thermogravimetric data (TG, Figure S5) constitute three-step thermograms for both TP and CT-1 MSs, mainly corresponding to the decomposition behaviors of TP. The new endothermal peak appears at 474.4 °C in the differential scanning calorimetry thermogram (DSC, Figure S5) of CT-1 MSs, indicative of the enhanced thermal stability.

TP oxidation and complexation with various metal ions including $Cu^{2+}$ have been widely investigated.[9,11b,c] To the best of our knowledge, no instance of forming such CT-1 MSs has been documented. The elevating temperature oxidation of TP in the presence of $Cu^{2+}$ should be important for the subsequent RT aggregation and assembly of oligo/polymeric TP into CT-1 spheres. Two control experiments of TP oxidation were thereby conducted for validation. One was oxidation of TP at RT in the presence of $Cu^{2+}$ (sample CT-0); the other was oxidation of TP at 100 °C without using $Cu^{2+}$ (sample T-0). CT-0 precipitates are macroscopic aggregates without definite shape (Figure S6A), and T-0 precipitates are also large, irregular aggregates (Figure S6B). Accordingly, these comparative results uncover the critical synergetic effects of temperature and Cu(II) on extending the interflavan linkages which enhance the hydrophobic π stacking interactions, leading to the assembly of oligo-/polymeric TP spheres. We present below the results obtained further by changing the combination of oxidation temperature and $Cu^{2+}$ concentration.

Figure 2A shows the sample obtained in the presence of 70 mM $Cu^{2+}$ at 70 °C (sample CT-2). Compared to CT-1 MSs,

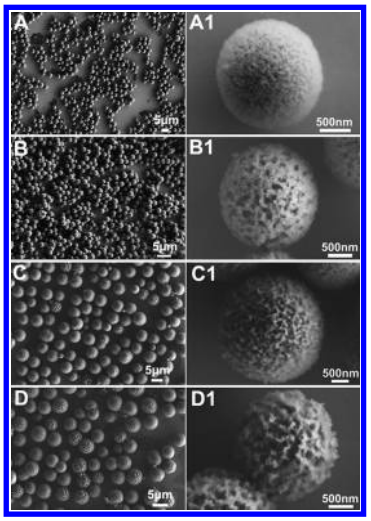


**Figure 2.** SEM images of TP spheres obtained at different reaction conditions: (A) CT-2, in the presence of 70 mM $Cu^{2+}$, at 70 °C; (B) CT-3, in the presence of 40 mM $Cu^{2+}$, at 70 °C; (C) CT-4, in the presence of 70 mM $Cu^{2+}$, at 50 °C; (D) CT-5, in the presence of 40 mM $Cu^{2+}$, at 50 °C. (A1−D1) SEM images of the single representative sphere of CT-2 to CT-5.

CT-2 are smaller spheres, ranging from 1.5 to 1.9 μm, with rough surface as indicated by discernible pores of tens of nanometer in size. CT-3 are monodisperse spheres with the average size of 2.05 μm (Figure 2B), which were also prepared at 70 °C but with a lower $Cu^{2+}$ concentration 40 mM. Their roughening extent further aggravates. Figure 2C shows the microspheres (sample CT-4) with average size of 2.0 μm obtained in the presence of 70 mM $Cu^{2+}$ at 50 °C. Pores with hundreds of nanometer in size are clearly distributed on the surface of CT-4 MSs. Sample CT-5 was prepared in the presence of 40 mM $Cu^{2+}$ at 50 °C, and the spheres have average size of 1.9 μm with porous spherical surface (Figure 2D). It is plausible that the nanopores distributed on CT-2 MSs gradually expand into a porous network structure on the roughening surface of CT-5 MSs. These results confirm that temperature and $Cu^{2+}$ concentration are two key factors in governing the structural/morphological evolution among oligo/polymeric TP spheres.

Figure 3A is the FE-SEM image of sample CT-6 obtained in the presence of 20 mM $Cu^{2+}$ at 50 °C. They are 700−850 nm hollow spheres (HSs), negatively charged (−36.4 mV) and


dx.doi.org/10.1021/ja311374b | J. Am. Chem. Soc. 2013, 135, 4179−4182

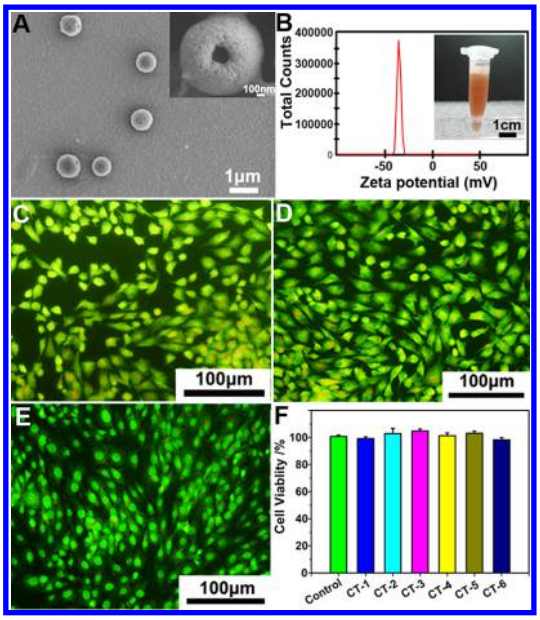


**Figure 3.** (A) SEM image of sample CT-6 obtained in the presence of 20 mM $Cu^{2+}$ at 50 °C, having a hollow type structure (inset). (B) Zeta potential distribution of CT-6 spheres in deionized water, indicating colloidable stability, e.g., in fetal calf serum (inset). Fluorescence micrographs of MG63 cells incubated with sample CT-1 for (C) 2 days, (D) 4 days and (E) 6 days. (F) MTT assays of MG63 cell viability incubated with different spheres.

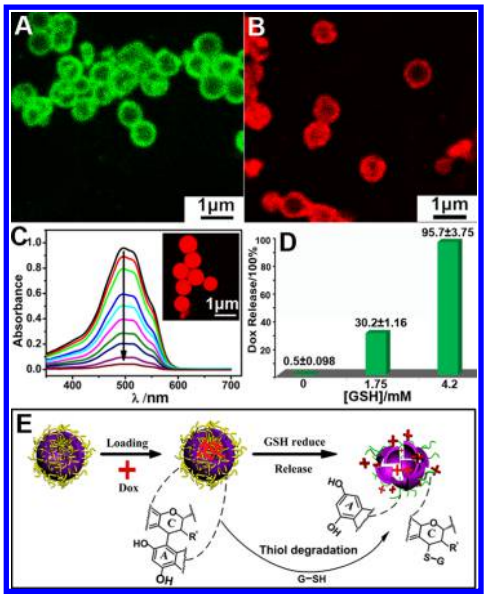


**Figure 4.** (A, B, inset in C) CLSM images of the CT-6 spheres loaded with FITC, Rhodamine B and Dox (at 543 nm). (C) UV−vis spectra of Dox solution (54 μg/mL, 1.5 mL) with increasing amounts of CT-6 spheres (from top to bottom: 0, 39.6, 94.9, 203.6, 255.6, 316.6, 377.9, 425.2, 486.9, 518.8 μg). (D) Dox release data from Dox@CT-6 in the presence of different glutathione concentration. (E) Schemetic illustration of Dox loading and GSH-responsive release.

colloidally stable in aqueous media, including in fetal calf serum (Figure 3B and inset), further demonstrating the strong modulation capability of the present strategy in organizing oligo/polymeric TP spheres. TP is evidenced to inhibit enzyme activities and signal transduction pathways, resulting in the suppression of cell growth and induction of apoptosis in human cancer.[6] In terms of oxidized TP polymers, previous systematic evaluation data by using deoxyribose, NBT photoreduction, lipoxygenase and POV assays suggested that they were also an excellent antioxidant in all lipid and nonlipid systems and had no pro-oxidant activity.[12d] In the present approach, the spheres were formed in water without the aid of any other organics, templates or cross-linkers, thus avoiding complicated preparation steps and potential toxic precursors. MG63 human osteoblast-like cells were thereby used as a model cell to evaluate the cytocompatibility of the obtained oligo/polymeric TP spheres. Figure 3C−E is the representative fluorescence micrographs of MG63 cells incubated for 2, 4, 6 days with CT-1 MSs that contain 3.5 $\mu g\ mg^{-1}$ Cu, in contrast to 2.0 $\mu g\ mg^{-1}$ Cu of CT-6 HSs. These cells present normal polygonal or spindle-like shape, and increase in number with longer culturing intervals. MTT assay data show that MG63 cells incubated with all the six groups of spheres proliferate well (Figure 3F), indicative of good cytocompatibility.

The encapsulation and delivery of guest molecules for biomedical purposes are further investigated by using CT-6 HSs as a host. Fluorescein isothiocyanate (FITC), rhodamine B isothiocyanate (RB) and doxorubicin hydrochloride (Dox) were chosen as model guest species. FITC and RB are widely used fluoresceins for bioimaging, and Dox is one of the most effective chemotherapeutic anticancer drugs in the past 50 years. Figure 4A,B and Figure S7 show that the FITC and RB loaded CT-6 HSs are monodisperse green and red nanocapsules, suggesting that CT-6 HSs could be potentially used for bioimaging purposes. The inset in Figure 4C is the CLSM image of CT-6 HSs loaded with Dox molecules. The size of these Dox@CT-6 HSs (ca. 780 nm) is nearly the same with the bare CT-6 HSs, confirming that Dox was mostly encapsulated into the voids of CT-6 HSs. The Dox loading amount is easily adjusted by changing the used amount of CT-6 HSs and quantified by using UV−vis spectrophotometry (Figure 4C) with reference to the calibration curve (Figure S8). The maximal Dox loading amount is about 15.4 wt %. The high loading efficiency is achieved through the strong interaction of positively charged Dox molecules with negatively charged CT-6 HSs. Figure S9 indicates the efficacy of Dox@CT-6 HSs with varying Dox concentrations on the apoptosis of HepG2 cells, and the coexistence of some complete CT-6 spheres loaded with Dox is still discernible alongside cells with uptake of Dox.

Figure 4D is the Dox release results from Dox@CT-6 HSs in the absence or presence of a varying glutathione (GSH) concentration, measured at physiological condition for 36 h. Without GSH, a negligible amount of Dox (ca. 0.5 wt % of the totally loaded Dox) was detected. This minor amount of Dox was probably arisen from the loosely adsorbed Dox by CT-6 HSs. In contrast, in the presence of 1.75 mM GSH, the release amount increased up to 30.2%. When the GSH concentration was elevated to 4.2 mM, about 96% of the loaded Dox released. SEM observations (Figure S10) reveal the structural splitting of CT-6 HS in the presence of GSH, suggesting that GSH as reducing agent reverts the oligo/polymeric TP to original compounds, to some extent (Figure 4E). This depolymerization by thiolysis reaction is similar with the cleavage of C4−C8(6) interflavan linkages of proanthocyanidins into monomeric polyphenols and their thioether adducts,[10b,12f,16] indicative of the presence of procyanidins-like linkages in CT-6 HS. These data demonstrate that the Dox release from Dox@CT-6 HSs is GSH concentration-responsive. GSH is distributed widely in the cytosol of cells at varying concentrations. In most


dx.doi.org/10.1021/ja311374b | J. Am. Chem. Soc. 2013, 135, 4179−4182

of cells, the GSH concentration is below 2 mM, but in some cells, such as hepatocytes and tumor/cancer cells, this concentration can reach about 10 mM.[17] The present data show that the efficacious Dox release (>96 wt %) from the CT-6 HSs carriers prefers a higher GSH concentration. Moreover, CT-6 HSs can endure the tough condition of concentrated hydrochloric acid (HCl), but collapse in weak alkaline environment (pH~8.3) (Figure S11). This acid-resistant but alkali-responsive property makes them capable of delivering functional guest species through acid barrier to alkaline destination, thus offering another option to release guest molecules.

In contrast to the extensive studies of TP oxidation and structural characterization, we simply changed the combination of temperature and $Cu^{2+}$ concentration of TP aqueous solutions, and obtained smooth, porous and hollow spheres (main parameters summarized in Table S1). This structural/morphological evolution is correlated with the steady reduction of the polymerization degree, calculated from gel permeation chromatography, from sample CT-1 (smooth) to CT-6 (hollow). The sample CT-1 has the highest value of 275 due to the enhanced oxidation activity at elevated temperature and more $Cu^{2+}$ addition. Spectroscopic and thermal analyses confirm that these oligo/polymeric TP have different linkage structures with those formed in enzymatic oxidation of TP, e.g. theaflavins. When the temperature goes down to RT, the aggregation and assembly in water into smooth, porous and hollow spheres are driven by the enhanced molecular entanglements and intermolecular forces of the extending linkages, such as hydrophobic $\pi$ stacking interactions and H-bonds.

As one of the essential trace metal elements present in our diet, copper is necessary for human health because of its involvement in many myriad processes, including iron metabolism, antioxidant defense, neuropeptide synthesis, and immune function.[18] Copper-quercetin complex was shown to be much effective free radical scavengers than the free flavonoids,[9b] and the polymerized TP by Cu(II) mediated oxidation of EC and EGCG was also reported to have stronger anticancer properties than their unoxidized forms.[12c] The present strategy is also feasible to prepare oxidized TP spheres by using other metals. The relevant spheric products obtained in the presence of other M-TP (M = Fe, Zn and Ag) are given in Figure S12. These spheres are in the range of 200−550 nm.

In summary, we have demonstrated a simple, template-free method to fabricate biocompatible functional spheres from naturally reproducible and edible green tea polyphenols in complete aqueous media. They could be smooth, porous and hollow spheres, simply by changing the temperature and $Cu^{2+}$ concentration of TP solutions. The TP hollow spheres were investigated for loading of guest species, including fluorescein and anticancer drug. These spheres are self-luminescent and stimuli-responsive including GSH responsive, acid resistant but alkali-responsive, suitable for potential biomedical purposes. With green tea polyphenols of beneficial health effects[6] as primary building units of spheres, the potential assistant therapeutic effects of these inornate objects are expected to be investigated on the basis of fully structural characterization.

## ■ ASSOCIATED CONTENT

### Supporting Information

Experimental details and the supporting figures. This material is available free of charge via the Internet at http://pubs.acs.org.

## ■ AUTHOR INFORMATION


### Corresponding Author

xli20004@yahoo.com


### Notes

The authors declare no competing financial interest.

## ■ ACKNOWLEDGMENTS

This work is supported by the National Basic Research Program of China (No. 2012CB933600).

## ■ REFERENCES


(1) (a) Langer, R. *Nature* **1998**, *392*, 5. (b) Imaz, I.; Hernando, J.; Ruiz-Molina, D.; Maspoch, D. *Angew. Chem., Int. Ed.* **2009**, *48*, 2325.

(2) Ma, N.; Li, Y.; Xu, H.; Wang, Z.; Zhang, X. *J. Am. Chem. Soc.* **2010**, *132*, 442.

(3) Ryu, J. H.; Chacko, R. T.; Jiwpanich, S.; Bickerton, S.; Babu, R. P.; Thayumanavan, S. *J. Am. Chem. Soc.* **2010**, *132*, 17227.

(4) Svenson, S.; Tomalia, D. A. *Adv. Drug Delivery Rev.* **2005**, *57*, 2106.

(5) Wei, W.; Ma, G. H.; Hu, G.; Yu, D.; Mcleish, T.; Su, Z. G.; Shen, Z. Y. *J. Am. Chem. Soc.* **2008**, *130*, 15808.

(6) (a) Yang, C. S.; Lambert, J. D.; Ju, J.; Lu, G.; Sang, S. *Toxicol. Appl. Pharmacol.* **2007**, *224*, 265. (b) Yang, C. S.; Wang, X.; Lu, G.; Picinich, S. C. *Nat. Rev. Cancer* **2009**, *9*, 429.

(7) (a) Jeong, B. C.; Kim, B. S.; Kim, J. I.; Kim, H. H. *J. Endourol.* **2006**, *20*, 356. (b) Chen, Z.; Wang, C.; Zhou, H.; Sang, L.; Li, X. *CrystEngComm* **2010**, *12*, 845−852.

(8) (a) Aron, P. M.; Kennedy, J. A. *Mol. Nutr. Food Res.* **2008**, *52*, 79. (b) Quideau, S.; Deffieux, D.; Douat-Casassus, C.; Pouységu, L. *Angew. Chem., Int. Ed.* **2011**, *50*, 586. (c) Li, N.; Taylor, L. S.; Ferruzzi, M. G.; Mauer, L. J. *J. Agri. Food Chem.* **2012**, *60*, 12531.

(9) (a) Jurasekova, Z.; Torreggiani, A.; Tamba, M.; Sanchez-Cortes, S.; Garcia-Ramos, J. V. *J. Mol. Struct.* **2009**, *918*, 129. (b) Bukhari, S. B.; Memon, S.; Mahroof-Tahir, M.; Bhanger, M. J. *Spectrochim. Acta, Part A* **2009**, *71*, 1901. (c) Pirker, K. F.; Baratto, M. C.; Basosi, R.; Goodman, B. A. *J. Inorg. Biochem.* **2012**, *112*, 10.

(10) (a) Pourcel, L.; Routaboul, J. M.; Kerhoas, L.; Caboche, M.; Lepiniec, L.; Debeaujon, I. *Plant Cell* **2005**, *17*, 2966. (b) Lakenbrink, C.; Engelhardt, U. H.; Wray, V. *J. Agric. Food Chem.* **1999**, *47*, 4621. (c) Tanaka, T.; Matsuo, Y.; Kouno, I. *J. Agri. Food Chem.* **2005**, *53*, 7571. (d) Haslam, E. *Phytochemistry* **2003**, *64*, 61.

(11) (a) Feldman, K. S.; Quideau, S.; Appel, H. *J. Org. Chem.* **1996**, *61*, 6656. (b) Torreggiani, A.; Jurasekova, Z.; Sanchez-Cortes, S.; Tamba, M. *J. Raman Spectrosc.* **2008**, *39*, 265. (c) Danilewicz, J. C. *Am. J. Enol. Vitic.* **2003**, *54*, 73.

(12) (a) Mochizuki, M.; Yamazaki, S.; Kano, K.; Ikeda, T. *Biochim. Biophys. Acta* **2002**, *1569*, 35. (b) Guyot, S.; Vercauteren, J.; Cheynier, V. *Phytochemistry* **1996**, *42*, 1279. (c) Azam, S.; Hadi, N.; Khan, N. U.; Hadi, S. M. *Toxicol. in Vitro* **2004**, *18*, 555. (d) Li, C. M.; Xie, B. J. *J. Agric. Food Chem.* **2000**, *48*, 6362. (e) Tanaka, T.; Matsuo, Y.; Kouno, I. *Int. J. Mol. Sci.* **2010**, *11*, 14. (f) Jiang, H. Y.; Shii, T.; Matsuo, Y.; Tanaka, T.; Jiang, Z. H.; Kouno, I. *Food Chem.* **2011**, *129*, 830.

(13) Oyama, K.; Yoshida, K.; Kondo, T. *Curr. Org. Chem.* **2011**, *15*, 2567.

(14) (a) Tsuchida, E.; Nishide, H.; Nishiyama, T. *Die Makromol. Chem.* **1975**, *176*, 1349. (b) Saito, K.; Kuwashiro, N.; Nishide, H. *Polymer* **2006**, *47*, 6581.

(15) (a) Coates, J. In *Encyclopedia of Analytical Chemistry*; Meyers, R. A., Ed.; John Wiley & Sons Ltd: Chichester, 2000; pp 10815−10837. (b) Khulbe, K. C.; Matsuura, T.; Lamarche, G.; Kim, H. J. *J. Membr. Sci.* **1997**, *135*, 211.

(16) Tanaka, T.; Takahashi, R.; Kouno, I.; Nonaka, G. *J. Chem. Soc., Perkin Trans.* **1994**, *1*, 3013.

(17) Minotti, G.; Menna, P.; Salvatorelli, E.; Cairo, G.; Gianni, L. *Pharmacol. Rev.* **2004**, *56*, 185.

(18) Harvey, L. J.; Ashton, K.; Hooper, L.; Casgrain, A.; Fairweather-Tait, S. J. *Am. J. Clin. Nutr.* **2009**, 2009S.